

Detailed Progress Report (UFR-56322)

Project title: Effect of ion irradiation on nanostructured Transition metal dichalcogenide systems.

A. 2014-2015 (FUC and report submitted before)

The approval letter for the aforesaid project was received in September 2014. After following the general procedures the project fellow was selected and the fellow (Mr. Saurabh Jyoti Hazarika) joined in the department on 30-09-2014. Apart from the relevant literature survey, a few experimental works related to the transition metal dichalcogenides based on synthesis of TiS_2 nanostructures have been carried out. The structural and optical properties have been studied.

A.1 Synthesis of TiS_2 nanoparticles:

The TiS_2 nanoparticles and nanosheets have been prepared using conventional hydrothermal method where TiCl_4 (LobaChemie, 99.5% pure) is used as the titanium source and anhydrous Na_2S as the sulphur source while tetrahydrofuran (THF) (THF, Rankem, 99.7% pure) was taken as the desired solvent being a polar solvent, [1]. The powder obtained is labelled as S_1 . The samples are then dispersed in a low molecular weight polymer (PVA) and are cast in glass slides. The sample is labelled as S_2 . The samples were subjected to 80 MeV- N^{4+} ion beams irradiation in the Material Science chamber under a high vacuum (pressure of 10^{-6} mbar) condition with a beam current of 1 pA, particle-nanoampere by varying the ion fluence as 5×10^{11} ions/cm², 5×10^{12} ions/cm² and 5×10^{13} ions/cm² and accordingly the samples were named as S_3 , S_4 and S_5 .

A.2 Results and discussion

(A) XRD analysis of nano- TiS_2 (irradiated and unirradiated):

The diffractogram of the pristine samples (S_1 , S_2) and the samples irradiated (S_3 , S_4 , S_5) at different fluences are shown in figure 1. In sample S_1 , the diffraction peaks positioned at $2\theta \sim 15.30^\circ$, 34.31° , 44.34° , 53.51° and 65.35° correspond to the hexagonal phase of TiS_2 (Figure 1(a)) (JCPDS card no. 74-1141) [2]. Most of the crystallites are believed to have preferential orientation along the (011) plane. A suppressed NaCl peak at $\sim 31.80^\circ$ is also seen. Moreover, a small peak at $\sim 48.20^\circ$ corresponds to the anatase phase of TiO_2 [3].

On the other hand, for the TiS_2/PVA system (S_2), the peaks for TiS_2 are observed at $2\theta \sim 15.35^\circ$, 34.12° , 44.15° and 65.25° along with the characteristic crystalline peak of PVA observable at $2\theta \sim 20.30^\circ$ [4] (Figure 4(b)). The average crystallite size has increased upon irradiation and decrease in

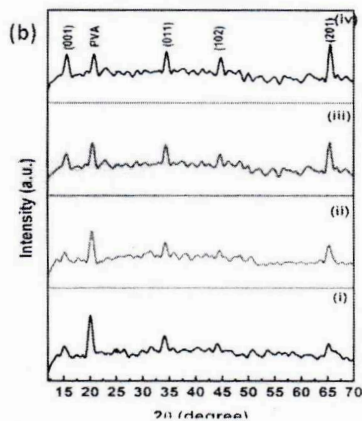


Fig 1 (a) XRD pattern of the sample S_1 , (b) XRD patterns of the samples S_2 (i), S_3 (ii), S_4 (iii) and S_5 (iv)

the full width half maxima (FWHM) value reveals an enhanced crystallinity for the irradiated samples, which can be explained by the fact that with the impact of high energetic ions on to the PVA films the polymer gets destroyed, allowing TiS_2 nanoparticles free from encapsulation (figure. 1 (b)). These irradiation induced free particles can agglomerate and make a bigger particle and thus increasing the grain size [5]. Using single line fitting (De-Bye Scherrer formula), the average crystallite size of the unirradiated sample and the irradiated samples are found to be approximately 8.52 nm (S_2) and 9.04 nm, 9.69 nm and 10.63 nm for S_3 , S_4 and S_5 respectively.

(ii) Morphological analyses through electron microscopy imaging :

Figure 2 (a) shows the TEM and SEM micrograph of a thin sliced specimen of the sample S_1 . The formation of TiS_2 nanosheets along with foldings is seen. Further magnified image highlights bilayer and multilayers sheets.

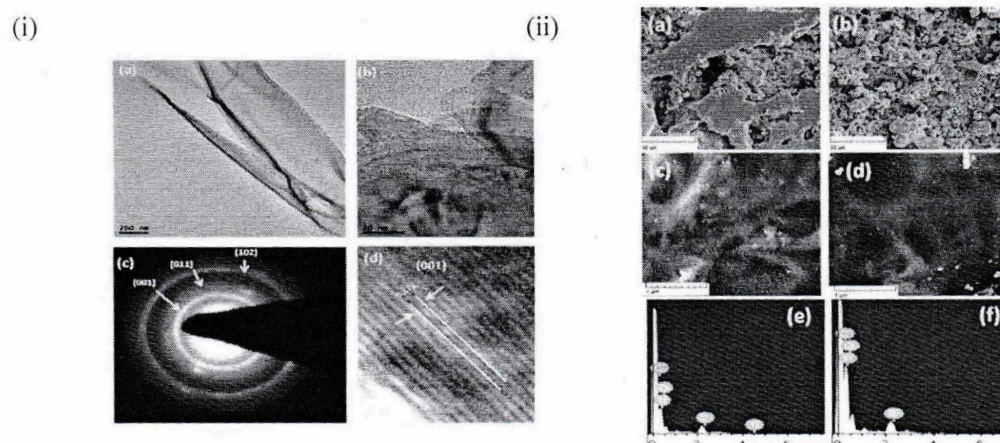


Fig 2: (i) TEM and SAED pattern of the sample S_1 (ii) FESEM images of the samples (a,b) S_2 , (c,d) S_4 and EDX micrographs of the samples (e,f) S_2 , (f) S_4

The interlayer separation of TiS_2 is ~ 0.57 nm, which is in good agreement with the literature value for the (001) plane of TiS_2 [6]. With irradiation, the size of the TiS_2 particles is enhanced as evident from the FESEM image. The EDX spectrum of the pristine sample (S_1) reveals a proportionately high intense S- peak along with Ti- peak and suppressed Na and Cl peaks. Quantitatively, Ti to S atomic percentage ratio is nearly 1:2, as desired for the development of TiS_2 . Whereas, the presence of C, O, Ti and S can be ensured from the EDX spectrum of the irradiated TiS_2 system.

(iii) UV- Visible optical absorption spectroscopy analysis:

Fig. 3 (a) gives the UV-Vis spectra for the pristine and the irradiated samples. An absorption peak at ~ 596 nm for the pristine sample can be ascribed due to $\text{M}^{2+} - \text{M}^{1+}$ of TiS_2 transition [7]. As we increase the fluence of the irradiated samples, we observed a red shift in the absorption edge, which leads to the decrease in the bandgap of the TiS_2 film. Using the Tauc's relation, the optical band gap

E_g is calculated for the direct and allowed transitions [8]. From the Tauc's plot (Fig. 3 (b)) the bandgap of the unirradiated sample (S_2) was found to be 2.85 eV and the value was found to decrease with increase in the ion fluence, as 2.34 eV, 1.97 eV and 1.79 eV for the samples S_3 , S_4 and S_5 ; respectively. The decrease in the band gap of the irradiated sample may be due to the increase in the crystallite size of the samples [9] leading to enhanced conduction of electrons in the irradiated films [10].

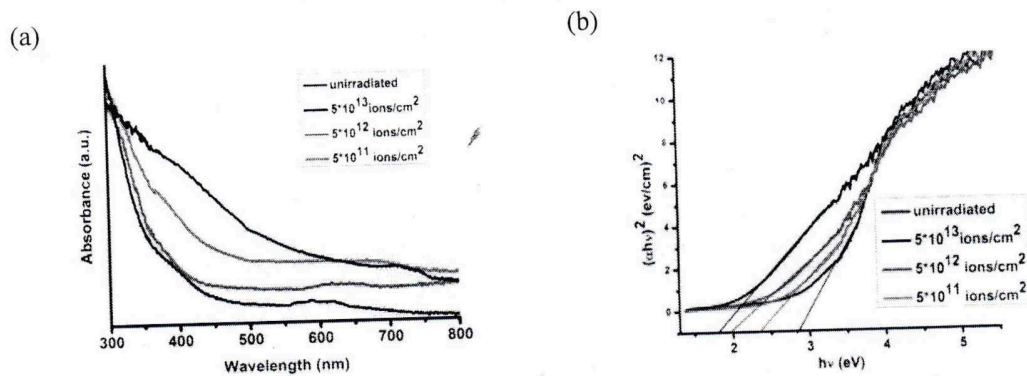


Fig 3 (a) UV absorption spectra and (b) Tauc's plot of the samples S_1 , S_2 , S_3 and S_4 .

B. 2015-2016 (FUC and report submitted before)

B.1 Synthesis of WS_2 nanoparticles:

We have attempted two hydrothermal methods for the production of WS_2 . In the first method we have taken sodium tungstate ($Na_2WO_4 \cdot 2H_2O$) as the source of tungsten and thiourea (CH_4N_2S) as the source of sulphur. The resultant product was blonde yellow in colour (labelled as S_1) and resembles to that of an intermediate product (WO_{3-x}) in the formation of WS_2 which is due to the inadequacy of sulphur in the reaction process. Here, we considered a second method where a solution of thiourea and deionized water was added to S_1 , yielding the product as S_2 .

B.2 Results and discussion

(i) XRD analysis :

The diffractogram of the WS_2 are shown in Figure 4. The XRD patterns of the as prepared samples are shown in figure 2. It can be seen that the sample S_1 , exhibits diffraction peaks which is similar to that of $WO_3 \cdot 5H_2O$ (JCPDS File No. 44-0363) and $WO_3 \cdot 33H_2O$ (JCPDS File No. 35-1001). For S_2 the peak at 14.32° corresponds to (002) plane of hexagonal WS_2 (JCPDS No. 08-

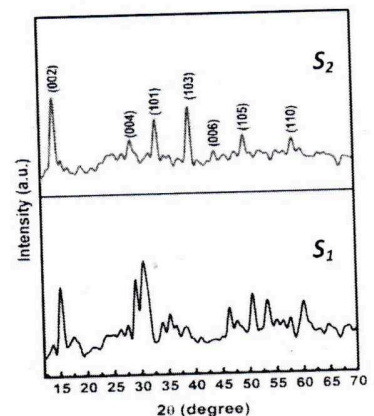


Fig 4: XRD pattern of the samples S_1 and S_2

0237) [11]. The other peaks at 29.28° , 35.79° , 39.57° , 44.28° , 49.85° , 55.53° , 60.16° and 65.19° also correspond to (004), (102), (103), (006), (105), (106), (008) and (114) planes of hexagonal WS_2 respectively. Using the Debye-Scherrer formula, we have calculated the average crystallite size of sample S_2 as 8.8 nm.

(B) Morphological analyses through electron microscopy imaging :

Fig. 5 shows the electron micrographs and EDX spectra of the sample 2. We can clearly see the formation of nano platelets along with some particles. The particles as well as the nano platelets are found to agglomerate and form clusters. The TEM image of the sample S_2 is shown in the fig. The formation of inorganic fullerene (IF) type particles can be observed from the fig 2 [12]. The average size of the IF type particles are found to be about 16 nm. The interlayer spacing is found to be 0.62 nm (fig. c). The formation of diffused rings in the SAED micrograph (fig. d) suggests the polycrystalline nature of the synthesized particles. The presence of elements W and S can be witnessed in the EDX spectrum of the sample S_2 .

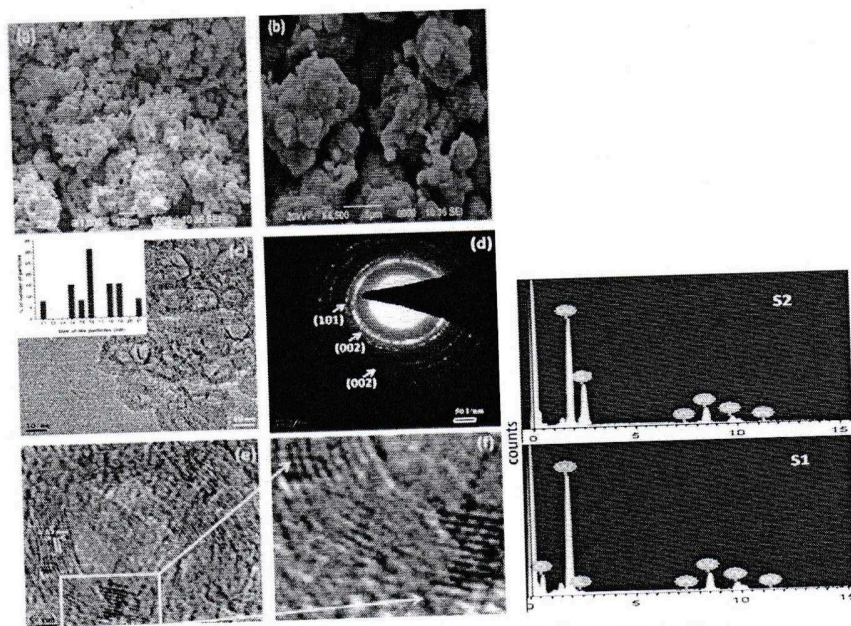


Fig 5: (a) Electron micrographs and EDX spectra of WS_2 nanosystems

(iii) Optical band gap calculation and luminescence response:

The UV-Vis optical absorption spectrum of the sample S_2 is shown in Fig. 6a. It depicts the presence of two weak absorption bands located at ~ 537 and ~ 649 nm. Even though these two bands represent characteristic absorption responses of IF- WS_2 nanostructures [13, 14], particularly the peak at ~ 649 nm corresponds to $d-d$ type transitions of the WS_2 at the center of the Brillouin zone [15]. In order to determine the band gap of the prepared WS_2 nanoparticles, we have plotted the Tauc's plot using the relation [16], $\alpha h\nu = (h\nu - E_g)^n$, where h is the Planck's constant, ν is the frequency of the incident light and α is the absorption coefficient. Putting $n = 1/2$ for the direct allowed transitions, the band gap of

the prepared WS₂ nanosystem is estimated to be 1.91 eV, which is in good agreement with an earlier report [17].

Figure 6b shows the PL spectrum of the synthesized WS₂ nanosystem acquired under an excitation wavelength of $\lambda_{exc} = 460$ nm. The broad peak at ~ 638 nm is the outcome of transition from the indirect band gap type to the direct band gap one when the bulk system is thinned down to a few nanometric layers [18]. This peak suggests the separation efficiency of the electron-hole pairs, with superior characteristics due to the presence of surface area and active edges [19]. Reports suggest that a direct gap exists at the K points of the Brillouin zone between the spin-orbit split valence band and the doubly degenerate conduction band. The indirect band gap is known to form between a local conduction band which is minimum at the midpoint between C and K and the valence band, which is maximum at the C point [18]. The existence of the direct transition can be explained from excitonic radiative relaxation and accordingly, the appearance of PL peak has been observed at energies slightly lower than the direct band gap (2.05 eV) of nano-WS₂ [18]. The luminescence pattern is observed to be asymmetrically broadened and with a fullwidth half-maxima (FWHM) of approximately 183 meV. A broad emission peak suggests that, the transition from the indirect to direct nature of the gap is not discrete, but continuous over inseparable energy bands.

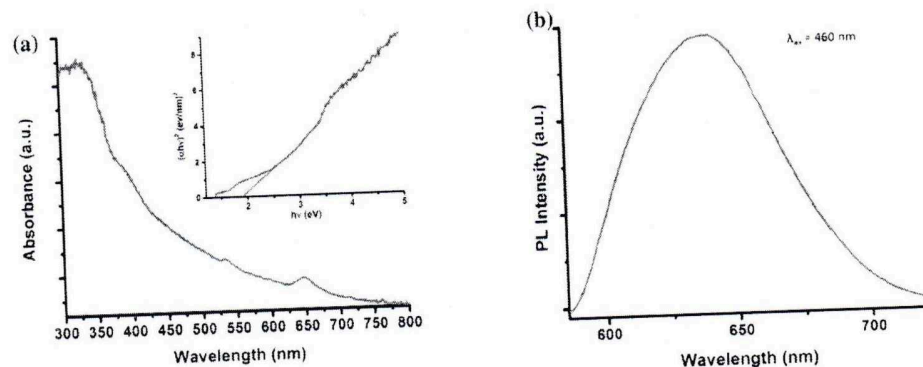


Fig. 6 (a) UV-Vis optical absorption spectrum along with the Tauc's plot (inset), and (b) PL spectrum of the IF nano-WS₂ system

(iv) Evaluation of photocatalytic performance of fullerene-type nano-WS₂ system:

To investigate photoactivity of the IF WS₂ nanoparticles, we have chosen MG as the target agent under UV and visible light illumination conditions. The UV-Vis absorption response of the organic dye and nano-WS₂ catalyst-loaded MG can be found in Fig. 7a. The WS₂ loaded dye showed a steady fall in the absorbance with increasing the UV exposure time, exhibiting a minimal strength at ~ 617 nm. Conversely, the samples irradiated under visible light showed a rapid drop in the absorbance response as compared to the samples subjected to UV light (Fig. 7(a), (b)). The IF WS₂ nanoparticles tend to exhibit better catalytic efficiency under visible light because of the narrow band gap, which

acts as a driving force to activate the redox reaction necessary for the production of hydroxyl radicals [17]. Also, it has been reported that irregular hexagonal-type structures with ample surface defects served the purpose of a good nanocatalyst under visible light illumination [16]. Also, IF-type particles can have enhanced photocatalytic responses because of the strong optical absorption, large surface area, and documented chemical inertness under illumination [20]. The schematic diagram as regards the mechanism of the photocatalytic activity of the synthesized WS₂ nanosystem is shown in Fig. 8.

The host WS₂ nanocatalyst, upon light irradiation would release electrons and holes. The excited electrons are likely to move to the conduction band creating adequate holes in the valence band. These generated charge carriers are likely to be trapped in the active W⁴⁺ and S²⁻ defect sites lest they might recombine with the counterparts to dissipate energy. These carriers would migrate to the nanocatalyst surfaces, resulting in the formation of reactive intermediates. The photoinduced holes and the reactive hydroxyl radicals are profoundly responsible for initiating the redox reaction required for decomposition of the harmful dye/organic pollutant. The hydroxyl radical is produced either by decomposition of water or by a hole reacting with the OH⁻. Since the target MG is in aqueous form; therefore, the water molecule is believed to come in contact with the surface of the nanocatalyst. The OH group or O²⁻ is likely to be trapped by the active sites of the nanocatalyst [21]. The oxygen vacancy centers are easily de-trapped and the electrons are transferred to the adsorbed oxygen which produces the superoxide radicals [22]. Water and hydroxyl ions are transformed to the hydroxyl radicals by the photo-generated holes [23]. These superoxide and hydroxyl radicals being very strong oxidizing agents could easily degrade the complete dye to its constituent products [24]. We observed an increasing trend of degradation of the MG on increasing the irradiation time. As high as 45% decomposition has been witnessed on irradiating the catalyst loaded dye under UV light for 120 min (Fig. 7c). Conversely, the IF-WS₂ nanocatalyst gives a superbly enhanced decomposition of MG (~71.2%) when subjected to visible light irradiation for 120 min (Fig. 7c). The performance of IF-type WS₂ nanosystem on the degradation of MG dye is evaluated through the simple kinetics, as discussed below. The kinetics of photocatalytic degradation of MG at the nanocatalyst surface can be understood through Langmuir–Hinshelwood (L-H) model [25]. For a dilute solution (mM) ($C \ll 1$), it can be expressed in the form of a first-order reaction given by [25]: $C_t = C_0 e^{-k_a t}$. Here, C_0 is the initial concentration of the MG solution, t is the irradiation time and k_a is the pseudo-first order rate constant. At $t = t_0$, $C = C_0$, the initial concentration of the target before irradiation. The percentage degradation of MG is represented in Fig. 7c. The plots of C_t/C_0 versus t , for UV and visible light conditions are shown in Fig. 7d. The plots essentially help to predict the pseudo-first-order rate constant, k_a . The rate constants, as obtained directly from the graphs (Fig. 7d), are calculated to be 0.0239 and 0.0414 min⁻¹ for IF nano-WS₂ samples exposed to UV light and visible light, respectively. A higher rate constant for the latter case, suggests that our IF nano-WS₂ are capable of displaying improved photoactivity under visible light illumination than that of UV exposure.

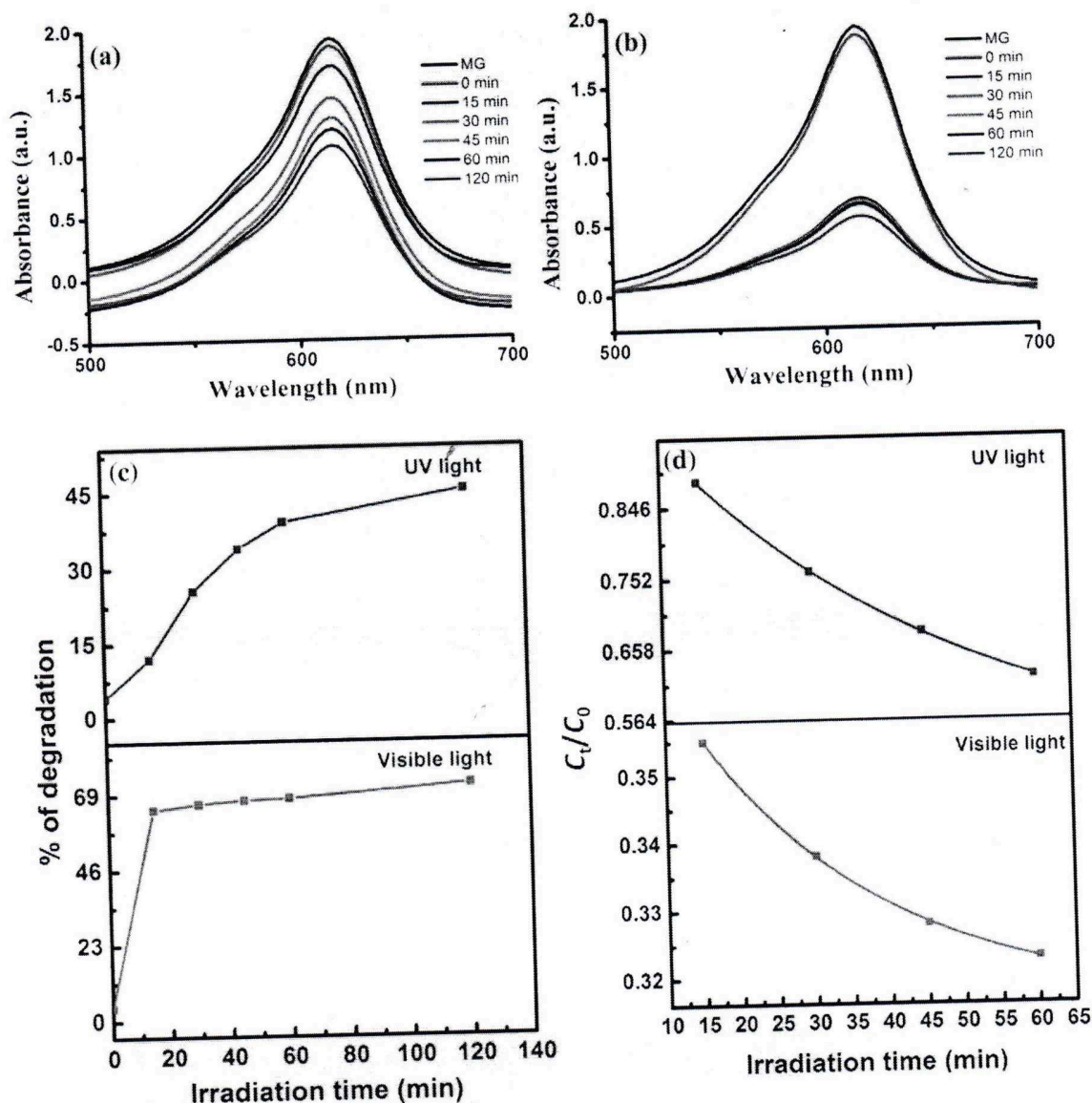


Fig. 7 UV-Vis absorption spectra of MG and IF nano-WS₂ catalyst-loaded dye with different irradiation times: a UV illumination, b visible light illumination. The percentage of degradation and pseudo-first-order plots under aforesaid conditions are shown in c, d on a comparative basis

C. 2016-17 (FUC and report submitted before)

C.1 Synthesis of WS₂ nanosheets:

First, a single-step hydrothermal process is attempted for the production of WS₂ and consequently, exfoliated into its nanosheets form with the help of repeated ultra-sonication. The chemicals used in the synthesis were of analytical grade and have been used without further purification. For synthesis, sodium tungstate (Na₂WO₄·2H₂O) (Rankem, 98% pure) is used as the source of tungsten, and thiourea (CH₄N₂S) (Merck, 99% pure) for sulfur. In a typical synthesis, 1.65 g of sodium tungstate, 0.72 g of hydroxylamine hydrochloride (NH₂-OH.HCl) (Merck, 98% pure) and 1.17 g of thiourea are dissolved in 30 ml of deionized Millipore® water. The solution is stirred for 1 h until a clear solution is obtained,

while maintaining the solution at pH=6. The mixture is then transferred into a 50 ml teflon-lined autoclave, and upon proper sealing, it is kept in oven at a temperature of 200 °C, for 24 h. After allowing it to cool naturally, the obtained product is washed several times with water and ethanol under centrifugation (~4000 rpm), for 10 min. The precipitate is oven dried at a temperature of 60 °C and consequently, a dark grey colored powder is acquired. The synthesized powder is labeled as S_1 .

To obtain nanosheets out of the synthesized WS_2 powder, 0.2 g of the powder is added to 20 ml of 1-methyl-2-pyrrolidone (NMP) (Merck, 99.5% pure) and then, subjected to ultrasonication bath for 4 h. The solution is then centrifuged (~5000 rpm) for 10 min and two-third of the solution is considered for further centrifugation (~7000 rpm) for 15 min, followed by multiple washing with ethanol. The as-received precipitate is collected and then oven dried (~60 °C) for a time duration of 10 h. The resulting product that yielded WS_2 nanosheets, is labeled as S_2 .

C.2 Results and discussion

XRD analysis of WS_2 nanosheets:

Fig.8 shows the XRD patterns of the as prepared WS_2 samples (un-exfoliated and nano-sheets). The samples exhibited diffraction peaks at nearly similar positions and no shift in the peak position has been observed. The diffraction peaks one positioned at $2\theta = 28.76, 33.42, 39.57, 44.28, 49.65$ and 58.53° correspond to (004), (101), (103), (006), (105) and (110) planes of the hexagonal (H) structure of WS_2 ; respectively [26]. The prominent peak, at $2\theta = 14.38^\circ$ refers to the (002) plane of $2H-WS_2$ (JCPDS File No.08-0237). The remarkable difference between the XRD patterns of the two samples is in the intensity of the peaks, with the nanosheets possessing a relatively lowered value due to lack of adequate atomic planes participating in the diffraction process. The lowering of the peak intensity is attributed to the decrease in the crystallinity of the nanosheets as compared to the unexfoliated WS_2 powder [27]. The diffraction peaks in the XRD pattern of the WS_2 sheets are also tend to get broadened, which suggest the exfoliation of the WS_2 powder into the sheets of nanoscale form [28]. No peak due either to impurities or oxide phase has been witnessed in the diffractograms, thus indicating formation of the phase pure WS_2 product in this case.

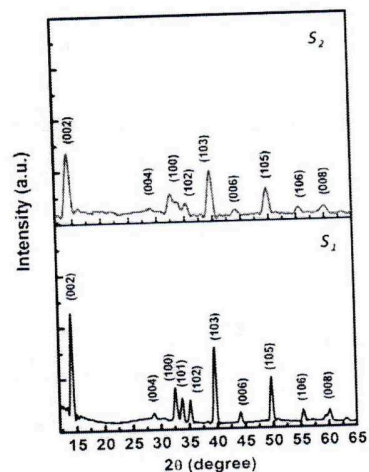


Fig 8: XRD pattern of the sample S_1 and S_2

(ii) Morphological analyses through electron microscopy imaging:

The micrographs of the un-exfoliated (S_1) and nanosheet (S_2) WS_2 powder captured on a HRSEM machine are shown in Fig. 9(a) and (b); respectively. Fig. 9B shows the EDX micrograph of the as synthesized WS_2 powder. The presence of the elements W and S can be clearly seen in the EDX spectrum. Intensity based calculations gave the ratio of S to W to be, 1.90:1.

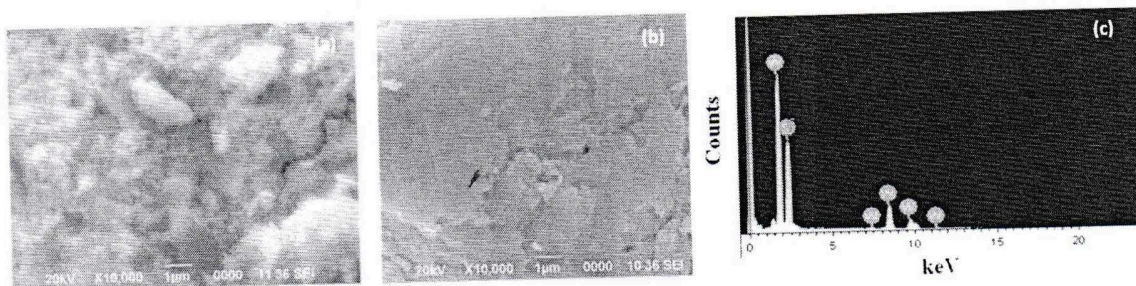


Fig 9: (a,b) HRSEM images of unexfoliated WS_2 and nanosheet; (c) EDX micrograph of WS_2 powder

Moreover, The exfoliated sheets are visualized at a higher magnification, through TEM imaging (Fig.10(a, b)). The nano-sheets, indicating high surface area coverage can be noticed with a few kinks and folds. The lattice fringe pattern captured at the edge of the WS_2 nanosheets being shown in Fig. 10(c). Using *ImageJ software*® [29], the average fringe width defining lattice spacing of the nanosheets has been calculated to be approximately, 0.62 nm. Moreover, the observation of diffused ring like pattern is an indicative of the polycrystalline content present in the synthesized WS_2 product (Fig. 10(d)).

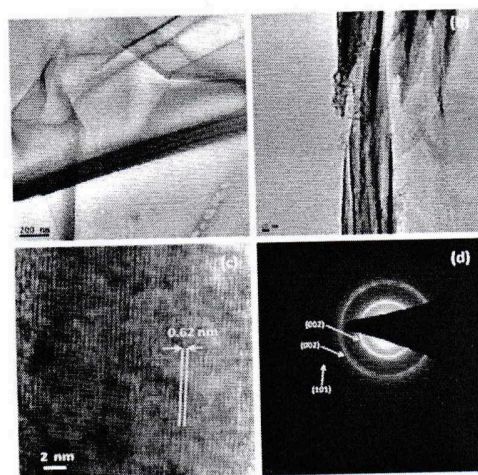


Fig 10 (a,b): TEM images of exfoliated WS_2 , (c) lattice fringes of WS_2 (d) SAED pattern of the polycrystalline WS_2 sample

(iii) BET surface area and pore size analysis using N_2 absorption-desorption curve

Surface analysis of nanoscale materials is an important aspect as it offers sound information as regards, surface coverage and particularly, specific surface area, pore size, pore volume etc. In this regard, earlier N_2 adsorption and desorption isotherms have been employed for studying mesoporous WS_2 [16]. The type of the isotherm is identified as type IV profile which is the characteristics of a

mesoporous material with pore diameters typically in the range of 2-50 nm [30]. Essentially, adsorption on mesoporous solids occurs via multilayer adsorption phenomena mediated via capillary condensation that results in type IV and V isotherms [31]. Here, Fig. 11 represents the characteristic N₂ adsorption/desorption isotherm of our hydrothermally processed and exfoliated WS₂ nanosheets. The initial part of the Type IV isotherm is attributed to the monolayer-multilayer adsorption since it follows the same trend as the corresponding part of a type II Isotherm obtained with the given adsorptive on the

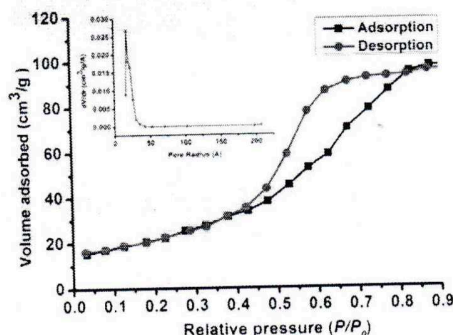


Fig.11 The nitrogen gas adsorption-desorption curve of the WS₂ nanosheets. The BJH pore size distribution curve is shown as inset

same surface area of the adsorbent in a non-porous form. The hysteresis loop is appeared to be of the type H₂ according to IUPAC classification which indicates disordered distribution of pore size and shape. The hysteresis loop is found to occur at a magnitude above ~ 0.5 of relative pressure P/P_0 . The BJH pore size distribution graph for the same sample is shown inside The BET surface area of the nano-sheets is found to be 211.5 m²/g. Using the BJH model, the pore volume and the average size of the pores are evaluated to be 0.433 cc/g and 3.8 nm respectively.

The Kelvin's equation [32] is:

$$\ln \frac{P}{P_0} + \frac{4\gamma V_m}{dRT} = 0 \quad (1)$$

where P and P_0 represent actual and saturated vapor pressures, V_m is molar volume, γ is the surface tension of liquid N₂ and $d (=2r, r$ being radius) is the size of the droplet. The symbols R and T signify universal gas constant (8.31 J-Mol⁻¹ K⁻¹) and working temperature (77 K); respectively. Putting the respective values, we obtain the diameter of the drop that desorb out of the pores as, $d=2r=2.1$ nm. However, a relatively larger pore size ($2r \sim 3.8$ nm) has been predicted through the experimental analysis and shown as inset of Fig. 11, which might have arisen due to the existence of interconnected pores on the surfaces of the nanosheets.

(iv) Synthesis of C dot-WS₂ hybridised systems:

Synthesis procedure: In a typical procedure, 20 ml of orange juice (absolutely pulp-free) was mixed with 15 ml ethanol in a beaker following an earlier work [33]. We have taken 10 ml of the as collected WS₂ supernatant and the 10 ml of the as prepared orange juice. The mixture was then carefully transferred into a 50 ml Teflon-lined stainless-steel autoclave and was heated at constant temperature of 120°C for 150 min. After the reaction is over, the autoclave was allowed to cool down naturally. A yellowish colour solution is obtained which show bluish green **fluorescence under UV excitation**.

Transmission Electron Microscopy (TEM) analysis

Fig. 12 shows the TEM micrograph of the as prepared 2D WS₂/ carbon dot hybrid system. We can clearly see the formation of dots over the nanosheets of WS₂. Further magnified images reveal the fringes of the 2D WS₂ nanosheets. The interplanar spacing of the WS₂ sheets were measured using *imagej* software and it is found to be 0.62 nm. Carbon dots are almost regular with size varying from 2 to 5 nm with *d spacing* of 0.34 nm. The CDs are formed on the surface of WS₂ without getting individually nucleated. The formation of the diffused rings is given from the SAED pattern which indicates the poly crystalline nature of the as prepared hybrid.

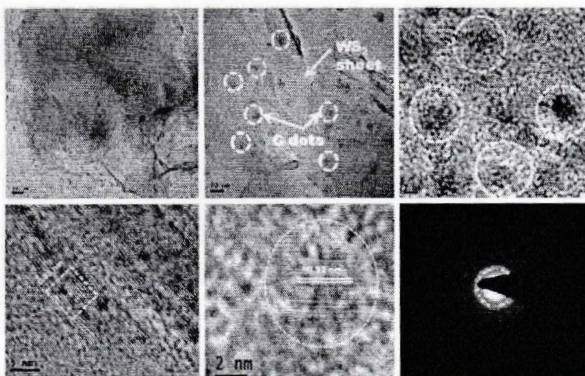


Fig 12: TEM micrographs of the CD/WS₂ hybrid system

Photoluminescence Spectra analysis

Fig. 13(a) depicts the PL spectra for both the synthesised WS₂ nanosheets (in black) and 2D WS₂/Carbon dot hybrid (in red) acquired under an excitation wavelength of $\lambda_{exc} = 360$ nm. We could observe a significant rise in the overall spectrum of the hybrid system, which is due to the presence of fluorophore (Carbon dot) in the WS₂. The PL spectra of WS₂ nanosheets and the WS₂/ C dot hybrid system share the same lineshape which reveal the effective interaction between WS₂ nanosheets and carbon dots in the hybrid system. Fig. 13(b) shows the excitation wavelength dependent PL spectra of the WS₂/ C dot hybrid system. When the excitation wavelength is changed from 350 nm to 450 nm the corresponding PL emission peaks for the hybrid system also changes from 450 nm (blue) to 531 nm (green). Also the intensities of the emission peaks found to decrease with increase in the excitation wavelength. However the upconverted PL property of the carbon dots which is reported to be an important reason to improve the photocatalytic activity of such kind of hybrid system was not found in this case [34]. Fig. 13(c) represents the optical micrographs of the WS₂/ Cdot hybrid under visible light and UV light illumination. The yellow coloured sample under visible light turns into blue under UV light. To further explore the fluorescent nature of the synthesized WS₂/ Cdot hybrid system, their fluorescent microscopy images have been taken which are shown in fig. 13(d). The images show the sample colours brown, blue, green and red when excited with white, ultraviolet, blue and green light respectively. The detailed analysis is still in progress.

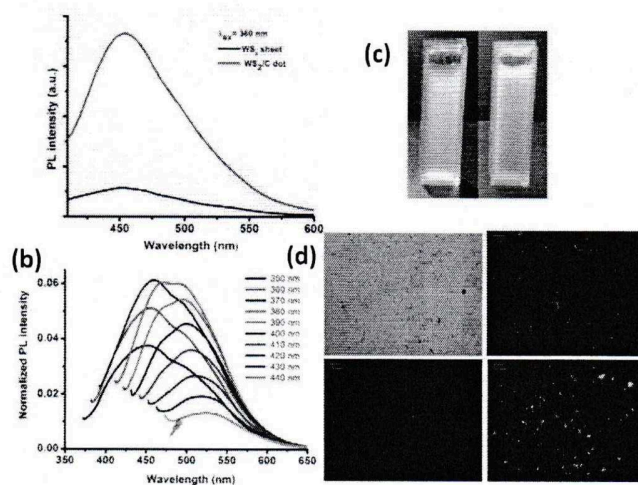


Fig 13: (a) PL spectra of unsynthesised WS₂ nanosheets and CD/WS₂ hybrid system (b) excitation dependent PL spectra of CD/WS₂ system (c) Optical micrographs of the hybrid system under visible and UV light (d) fluorescent microscopy images of the hybrid system

Acknowledgments

We acknowledge IUAC, New Delhi for the financial support (UFR-56322/2014) and thank them for providing good quality nitrogen beam and FESEM and EDX facilities.

We thank SAIC, TU, for extending TEM imaging facility. We also thank colleagues for valuable discussion and timely assistance.

References

1. Lu Z. et al. Nature Comm. 2, 213, 2011.
2. Wold A and Dwight K, J. Sol. St Chem., 96, 53-58, 1992.
3. Tan M, Wang Z, Peng J, and Jin X. Facile Synthesis of Large and Thin TiS₂ Sheets via a Gas/Molten Salt Interface Reaction. J. Am. Ceram. Soc. 98, 1423-1428, 2015
4. Ramchiary A, Samdarshi S K, Chem. Phys. Lett., 597, 63-68, 2014.
5. Attia G and Abd El-kader M F H, Int. J. Electrochem. Sci., 8, 5672, 2013.
6. Cao S, Liu T, Hussain S, Zeng W, Peng X, Pan F, Wilson J A and Yoffe A D, Adv. Phys., 18, 193, 1969.
7. Myron H W, Freeman A J, Phys. Rev. B, 9, 481, 1974.
8. Yang J, Voiry D, Joon Ahn S, Kang D, Kim A Y, Chhowalla M, Shin H S, Angew. Chem. Int. Ed. 52, 1-5, 2013
9. Mir F A, Rehman S, Asokan K, Khan S H, Bhat G M, J Mater Sci: Mater Electron, 25, 1258-2014.
10. Sheena P A, Priyanka K P, Sabu N A, Gannesh S and Varghese T, Bull. Mater. Sci., 38, 825-830, 2015.

11. Shang Y, Xia J, Xu Z, Chen W, J. Disp. Sci. Technol. 26, 635, 2005
12. Cao S, Liu T, Hussain S, Zeng W, Peng X, Pan F, Mater. Lett. 129, 205, 2014
13. Feldman Y, Frey G L, Homyonfer M, Lyakhovitskaya V, Margulis L, Cohen H, Hodes G, Hutchison J L, Tenne R, J. Am. Chem. Soc. 118, 5362, 1996
14. Frey G L, Elani S, Homyonfer M, Feldman Y, Tenne R, Phys. Rev. B 57, 6666, 1998
15. Notley S M, J. Coll. Interf. Sci. 396, 160, 2013
16. Vattikuti S V P, Byon C, Sci. Adv. Mater. 7(12), 2639, 2015
17. Sang Y, Zhao Z, Zhao M, Hao P, Leng Y, Liu H, Adv. Mater., 27, 363, 2015
18. Gutierrez H R, Perea-Lopez N, Elias A L, Berkdemir A, Wang B, Lv R, Lopez-Urias F, Crespi V H, Terrones H, Terrones M, Nano Lett. 13, 3447, 2013
19. Parshetti G, Kalme S, Saratale G, Govindwar S, Acta Chim. Slov. 53, 492, 2006
20. Tributsch H, Structure and bonding, vol. 49 (Springer, Berlin, 1982), p. 127
21. Paul N, Deka A, Mohanta D, J. Appl. Phys. 116, 144902-1-7, 2014
22. Bingham S, Daoud W A, J. Mater. Chem. 21, 2041, 2011
23. Parida K M, Sahu N, J. Mol. Catal. A 287, 151, 2008
24. Peng T, Zhao D, Song H, Yan C, J. Mol. Catal. A 238, 119, 2005
25. Gaya U I, Abdullah A H, J. Photochem. Photobiol. C 9, 1, 2008
26. Shang Y, Xia J, China Zhude Xu and Chen W, J. Disp. Sci. Technol., 26(5), 635, 2005
27. Mao X, Xu Y, Xue Q, Wang W and Gao D Nanoscale Res. Lett., 8 430, 2013
28. Lin H, Wang J, Luo Q, Peng H, Luo C, Qi R, Huang R, Travas-Sejdi J and Duan C-G J. Alloys Compd., 699, 222, 2017
29. <http://imagej.nih.gov/ij/>
30. AlOthman Z A Materials, 5, 2874, 2012
31. Kruk M and Jaroniec M, Chem. Mater., 13, 316, 2001
32. Butt H-J, Graf K and Kappl M 2006 "The Kelvin Equation". Physics and Chemistry of Interfaces (Weinheim: Wiley-VCH)
33. Sahu S, Behera B, Maiti T K and Mohapatra S, Chemical Communications, 2012
34. Zhang Z, Zheng T, Li X, Xu J, and Zeng H, Part. Part. Syst. Charact., 33, 457, 2016

OUTCOME

1. Presented poster at CM DAYS 27th-29th Aug, 2015, held at Visva-Bharati, Santiniketan.
2. Presented oral paper at CM DAYS 29th-31st Aug, 2016, held at Mizoram University.
3. Presented poster at NCHSCMP, 2nd-4th March, 2017, held at Tezpur University.
4. Presented poster at CM DAYS 29th-31st, Aug, 2017, held at Tezpur University.

5. Paper published in the Journal of Physics: Conference series, 765 (2016) 012007
doi:10.1088/1742-6596/765/1/012007.
6. S J Hazarika, D. Mohanta, Appl. Phys. A , 123:381, 2017.
7. S J Hazarika, D Mohanta, Bulletin of Material Science, 41:163 (2018).

FUTURE PLAN OF WORK:

- 1) To investigate the mechanical properties of the synthesized WS₂ nanostructures.
- 2) To study the effect of irradiation on these prepared systems.



FUND UTILIZATION CERTIFICATE

(PROJECTS/SCHEMES)

Name of the Nodal institution /

Department of Organisation : TEZPUR UNIVERSITY

Name of the project : "Effect of ion irradiation on nanostructured transition metal dichalcogenide systems"

Certified that an amount of Rs 1,09,467 of grant-in aid sanctioned during the financial year 2014-2015 in favour of the Registrar, Tezpur University on the subject **UFR-56322** project **IUAC**, New Delhi as per sanction order no. IUAC/XIII.7/UFR-56322 dated 22/08/2014 on the head of "contingency" and order no. IUAC/XIII.7/UFR-56322 dated 23/12/ 2014 on the head of "fellowship"; a sum of Rs. 1,12,240 has been utilized till 31st March, 2015.


Principal Investigator
Project Title : Effect of --- systems
Sponsor Agency : IUAC
Department of Physics
Tezpur University


Finance officer
Tezpur university
Finance Officer
Tezpur University

EXPENDITURE STATEMENT OF IUAC(UFR-56322) PROJECT

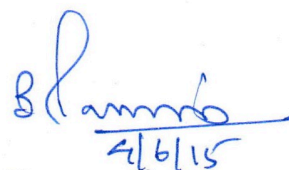
TITLE: "Effect of ion irradiation on nanostructured transition metal dichalcogenide systems"

Sl.no	Heads of account	Received grant(Rs.)	Expenditure during 2014-2015 (Rs.)	Balance (Rs.)
1.	Contingency	25,000	27,773	- 2,773
2.	Fellowships	84,467	84,467	0
	TOTAL	1,09,467	1,12,240	-2,773



Registrar

Tezpur University
Registrar
Tezpur University



Finance officer

Tezpur university
Finance Officer
Tezpur University

FUND UTILIZATION CERTIFICATE

(PROJECTS/SCHEMES)

Name of the Nodal institution /

Department of Organisation : TEZPUR UNIVERSITY

Name of the project : "Effect of ion irradiation on nanostructured transition metal dichalcogenide systems"

Certified that out of Rs 1,93,000 of grant-in aid sanctioned during the financial year 2015-2016 in favour of the Registrar, Tezpur University on the subject UFR-56322 project IUAC, New Delhi as per sanction order no. IUAC/XIII.7/UFR-56322 dated July 21, 2015; an excess expenditure of previous year ₹ 2773; a sum of ₹ 1,90,220 has been utilized till 31st March, 2016.

Principal Investigator

16.5.2016
Title: Effect of irradiation on system
Department of Physics
TEZPUR UNIVERSITY

Finance officer

Tezpur university
Finance Officer
Tezpur University

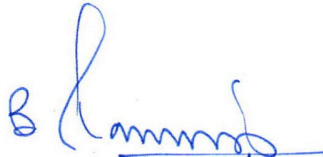
**STATEMENT OF EXPENDITURE OF IUAC (UFR-56322) PROJECT
(for the year 2015-16)**

TITLE: "Effect of ion irradiation on nanostructured transition metal dichalcogenide systems"

Sl.no	Heads of account	Opening balance (₹)	Received grant during 2015-16 (₹)	Net fund during 2015-16 (₹)	Expenditure during 2015-2016 (₹)	Balance (₹)
1.	Contingency	(-) 2773	25,000	22,227	22,220	7
2.	Fellowships	nil	1,68,000	1,68,000	1,68,000	0
	TOTAL	(-) 2773	1,93,000	1,90,227	1,90,220	7


Registrar

Tezpur University
Registrar
Tezpur University


Finance officer 20/5/16

Tezpur University
Finance Officer
Tezpur University

FUND UTILIZATION CERTIFICATE

(PROJECTS/SCHEMES)

Name of the Nodal institution /

Department of Organisation : TEZPUR UNIVERSITY

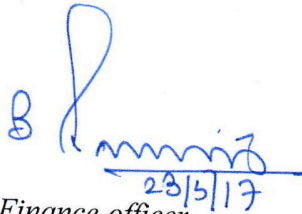
Name of the project : **“Effect of ion irradiation on nanostructured transition metal dichalcogenide systems”**

Certified that out of Rs 2,05,059 of grant-in aid sanctioned during the financial year 2016-2017 in favour of the Registrar, Tezpur University on the subject UFR-56322 project IUAC, New Delhi as per sanction order no. IUAC/XIII.7/UFR-56322 dated August 30, 2016; a sum of Rs 2,05,056 has been utilized till 31st March, 2017.


Principal Investigator

Principal Investigator
Title *Effect of ion irradiation on nanostructured transition metal dichalcogenide systems*

Department of *Physics*
TEZPUR UNIVERSITY


23/5/17
Finance officer

Tezpur university

Finance Officer
Tezpur University

**STATEMENT OF EXPENDITURE OF IUAC (UFR-56322) PROJECT
(for the year 2016-17)**

TITLE: "Effect of ion irradiation on nanostructured transition metal dichalcogenide systems"

Sl. No.	Heads of account	Unspent balance of previous grant (Rs.)	Received grant during 2016-17 (Rs.)	Net fund during 2016-17 (Rs.)	Expenditure during 2016-2017 (Rs.)	Unspent Balance (Rs.)
1.	Contingency	7	24,993	25,000	24,990	10
2.	Fellowships	nil	1,80,066	1,80,066	1,80,066	0
	TOTAL	7	2,05,059	2,05,066	2,05,056	10



Registrar

Tezpur University

**Registrar
Tezpur University**



Finance officer

Tezpur University

**Finance Officer
Tezpur University**

FUND UTILIZATION CERTIFICATE

(PROJECTS/SCHEMES)

Name of the Nodal institution /

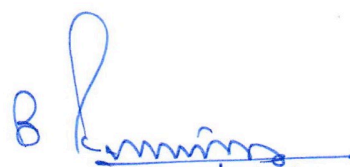
Department of Organisation : TEZPUR UNIVERSITY

Name of the project : "Effect of ion irradiation on nanostructured transition metal dichalcogenide systems"

Certified that out of Rs 95,457 of grant-in aid sanctioned during the financial year 2017-2018 in favour of the Registrar, Tezpur University on the subject UFR-56322 project IUAC, New Delhi as per sanction order no. IUAC/XIII.7/UFR-56322 dated September, 13, 2017; a sum of ₹ 95,457 has been utilized till 31st March, 2018.



Principal Investigator



Finance officer 30/5/18

Tezpur university
Finance Officer
Tezpur University

**STATEMENT OF EXPENDITURE OF IUAC (UFR-56322) PROJECT
(for the year 2017-18)**

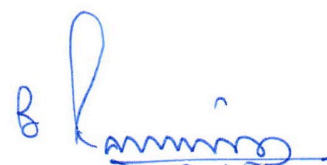
TITLE: "Effect of ion irradiation on nanostructured transition metal dichalcogenide systems"

Sl. No.	Heads of account	Received grant during 2016-17 (Rs.)	Expenditure during 2017-2018 (Rs.)	Unspent Balance (Rs.)
1.	Contingency	nil	nil	nil
2.	Fellowships	95,457	95,457	0
	TOTAL	95,457	95,457	0



Registrar

Tezpur University
Registrar
Tezpur University



Finance officer

Tezpur University
Finance Officer
Tezpur University